Chapter

Engineering the Color and the Donor-Acceptor Behavior in Nanowires: Blend Versus Coaxial Geometry

Mohamed Mbarek and Kamel Alimi

Abstract

The blending or the bilayering of two complementary species are the dominant methods for in-solution-processed thin film devices to get a strong donor-acceptor behavior. They propose opposite strategies for the respective arrangement of the two species, a central point for energy and/or charge transfer. In this work, we propose to engineer at the scale of the exciton diffusion length the organization of a donor (poly(vinyl-carbazole), PVK) and an acceptor (poly(para-phenylene-vinylene), PPV) in a nanowire geometry. A two-step template strategy was used to fabricate coaxial nanowires with PPV and PVK, alternatively as the core or the shell material. Their stationary and time-resolved photoluminescence properties were investigated and compared to the case of PVK-PPV blend. Their respective characteristics are direct evidences of the dominant mechanisms responsible for the emission properties.

Keywords: organic nanowires, luminophores, exciton, shell-core

1. Introduction

π-conjugated molecules and polymers have attracted considerable interest in both fundamental studies and applied research [1]. This is due to their one-dimensional characteristics and their many potential applications. One-dimensional (1D) nanostructures based on organic materials are attracting significant research [2–4] interest owing to the many novel chemical, physical, and electronic properties that may arise in such systems and the possibility of exploiting these properties in a variety of applications [5–9]. However, for 1D nanostructure in general, a key challenge is the development of new approaches that will permit controlled nanowires and nanotubes architectures [10]. Nanoporous template method has been used to synthesize well-defined nanoscale tubes or wires inside nanoporous channels [10, 11]. This technique has many advantages, in that it is low-cost, control of physical properties or size is easy [10, 11], and that it lends itself to the logic of mass production. The fabrication of nanoscale structures has attracted much interest due to their potential use in electronic and optical applications [12–16]. Among many techniques generating the nanoscale structures, the anodized aluminum oxide (AAO) [10, 11] has been most widely used as a template for forming metal or semiconductor nanowires. The AAO has been known to have a clear advantage of an economical way to produce the large area periodic nanostructures [11]. These

nanostructures were a seat of charge and energy transfer especially on the acceptor-donor architecture [17, 18]. The energy transfer [19] depend the absorption, the quantum yield of emitter's efficiency. Additionally, it depend on the donor and acceptor characters of luminophores, the relative spatial distribution of acceptor and donor, the overlapping between the donor absorption spectrum and the acceptor emission spectrum.

In this way, we report the synthesis of poly(para-phenylene-vinylene) PPV [20] (electron donor) and poly(vinyl-carbazole) PVK [20] (good hole transport) nanowires, and a coaxial architecture bases on PPV and PVK polymers using the AAO and describe their optical and structural characteristics. Stationary and transition photoluminescence have been employed to demonstrate the nature of energy and charge-transfer processes occurring in these nanostructures.

2. Materials and techniques

2.1 Materials

Poly(N-vinylcarbazole) PVK powder, chloroform, methanol, used for the synthesis of the studied compounds were purchased from Sigma Aldrich, Merk, and Fluka. The materials were used as received. The PPV precursor was synthesized by addition of 33 mL of tetrahydrothiophenium in the dichloroparaxylene dissolved in methanol. The aqueous solution of PPV precursor was dialyzed with deionized water for several days. The PPV precursor was kept at 0°C in the dark. The mass concentration of the PPV precursor is about 2.4 mg mL. Commercial AAO membranes purchased from Whatman (anodisc 13) have been used. They are 60 μm thick with a real pore diameter showing a polydispersity between200 nm and around 250 nm as revealed by SEM analysis.

2.2 Fabrication of the coaxial NWs

The coaxial NWs were fabricated by a wetting template method in anodic alumina oxide (AAO) nanoporous template. For the synthesis of coaxial NWs, two steps of wetting are required. The first step consists in the wetting of AAO membrane with the PPV precursor in methanol solution. To obtain PPV nanotubes, the concentration of PPV precursor in methanol was chosen at 1.2 mg/mL and 200 μL of this solution was drop-casted on AAO membrane, as described elsewhere. The precursor embedded in AAO membrane was then thermally converted under a dynamic secondary vacuum (≈10–6 Torr) for 4 h to obtain PPV. The coaxial nanowires are then obtained by a secondary-template strategy. The AAO membrane containing PPV nanotubes was wetted with the solution containing PVK dispersed in chloroform. The wetted templates were left overnight under ambient condition to allow solvent evaporation. For some characterization, the AAO templates containing coaxial NWs was completely etched in H3PO4 (25 wt %) overnight and washed several time with DI water. The coaxial NWs were homogeneously dispersed in DI water solution by ultrasonication during 10 s with a power of 140 W (Fisher Scientific FB 15052). Ultrasonication results in the shortening of the nanowire length.

3. Characterization methods

A field-effect scanning electron microscope (JEOL, JSM-7600F operating at 5 kV), an AFM (Nanowizard II, JPK instruments) working in intermittent contact

mode in air with Si tips (PPP-NCHR, Nanosensors) and a transmission electron microscope (Hitachi H9000 NAR operating at 300 kV) were used to investigate the morphology and the composition of the nanowires. For SEM, AFM and fluorescence microscopy experiments, a drop of solution (10 μL) containing the nanowires was deposited onto silicon or glass substrates after the dissolution of the template. For TEM experiments, a drop of the solution was deposited on TEM copper grids covered with a thin holeycarbon film. Epi-fluorescence micrographs were acquired using a calibrated microscope (Eclipse Ti, Nikon) equipped with a 60 objective and a CCD camera, 130WHg lamp and fluorescence filter cube (EX 330–380, Dm: 400, BA 420). Spectroscopic Characterizations.

All characterizations were performed at room temperature. Absorption and photoluminescence of the PVK were measured on spin coated thin films (1500 rpm, 30 s) deposited on glass and silica from a solution with 2.4 mg/mL-1, and from a PPV precursor (PPV precursor: 2.4 mg/mL-1 in methanol, 1500 rpm, 30 s, thermal conversion at 300°C for 3 h). UV–vis absorption on thin film sample was performed with a Perkin-Elmer double beam spectrophotometer equipped with an integrating sphere; we carried out PL measurements using a Jobin-Yvon Fluorolog 3 equipped with a CCD camera and PL experiments on film were achieved under 400 nm excitation at 0.5 mW by a Spectra-Physics Hurricane X laser. For micro-Raman and micro photoluminescence studies, the template containing the nanowires was broken to reveal a cross section and consequently the whole length of the nanowires. Micro-Raman spectra were recorded using a Renishaw inVia Raman microscope equipped with a 785 nm line of a HPNIR diode laser. We measured steady state micro-PL spectra with a Jobin-Yvon T64000 spectrometer under 325 nm laser excitation obtained by an argon ion laser. In each case, the spot size of the focused laser beam on the sample was estimated to be about 1.2 μm. The transient PL experiments have been achieved under 400 nm excitation using Spectra-Physics Hurricane X laser system (82 fs, 1 kHz) onto mat of NWs. The collected emission was temporally detected with a streak camera (Hamamatsu C7700) coupled with an imaging spectrograph. The laser pump power in pinging on sample was kept at 0.5 mW to minimize sample photobleaching.

4. Results and discussion

A selection of transmission electron microscopy (TEM) was performed to characterize the different nanowires based on PPV and PVK. The different types of TEM imaging and their correspondent's histograms are shown in the **Figure 1**.

A selection of transmission electron microscope (TEM) images of the as-prepared nanofibres after the dissolution of the AAO membrane is presented in **Figure 1**. The PPV nanofibres have a mean diameter d (272 nm) exceeding the nominal manufacturer pore diameter dp (200 nm) of AAO membrane as shown by the histograms. The same diameter was observed in the PVK nanowires displayed in TEM micrographs with a mean diameter d = 270 nm (**Figure 1b**) supported by their histograms nanowires diameters in the right of **Figure 1**.The nanowires length 10 μm does not correspond to the membrane thickness (60 μm), this difference can be explained by the alumina removal step and the sonication step required for their dispersion in solution, which result in shortening of the NWs.

We performed also transmission electron microscopy (TEM) and scanning electron microscopy experiments on the coaxial nanowires to make evidence of the coaxial architecture and to prove the successful synthesis of these coaxial nanostructures bases on PVK and PPV polymers. The poor imaging contrast typical of polymeric materials make not easy to prove that. In **Figure 2**.

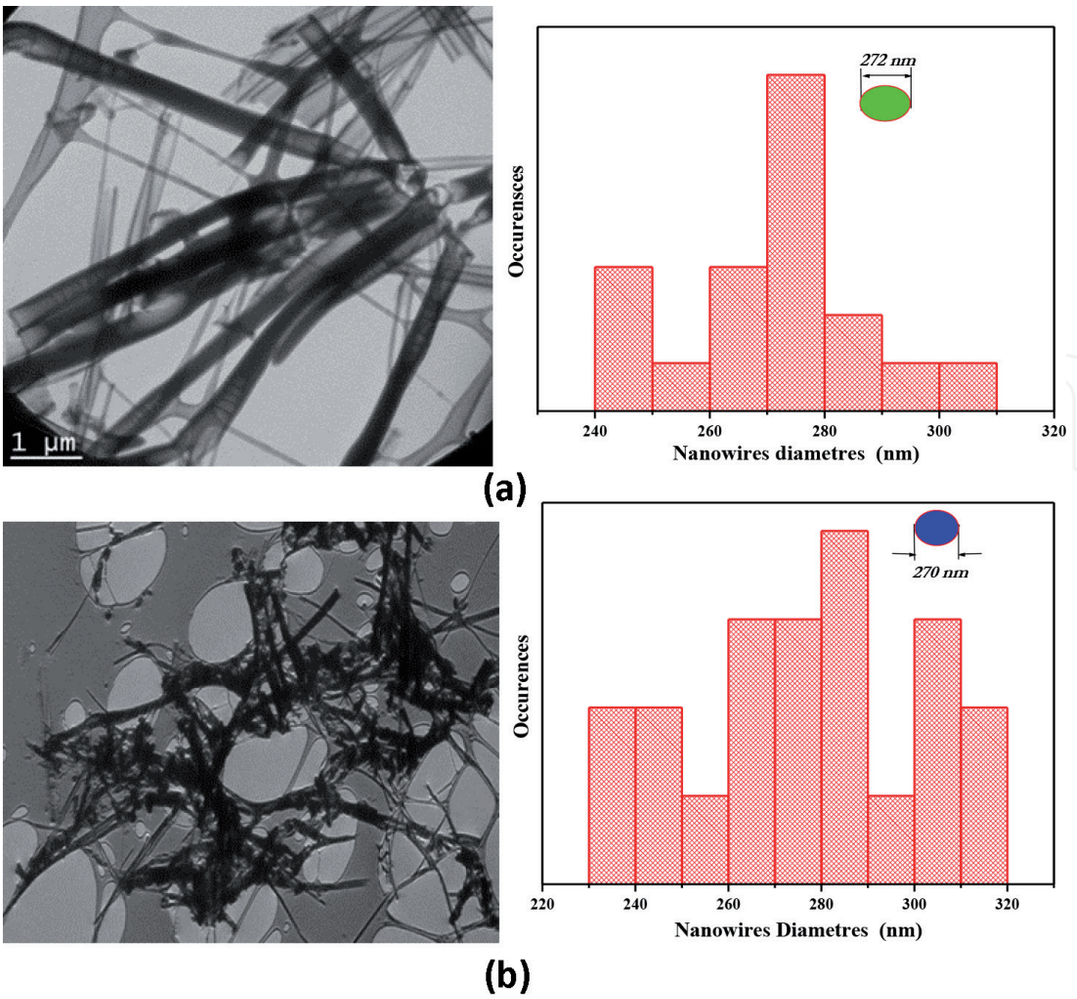

Figure 1.
Selection of TEM micrographs of: (a) PPV nanowires and it histograms nanowires diameters (right of TEM image), (b) of PVK nanowires and it histograms nanowires diameters (right of TEM micrograph).

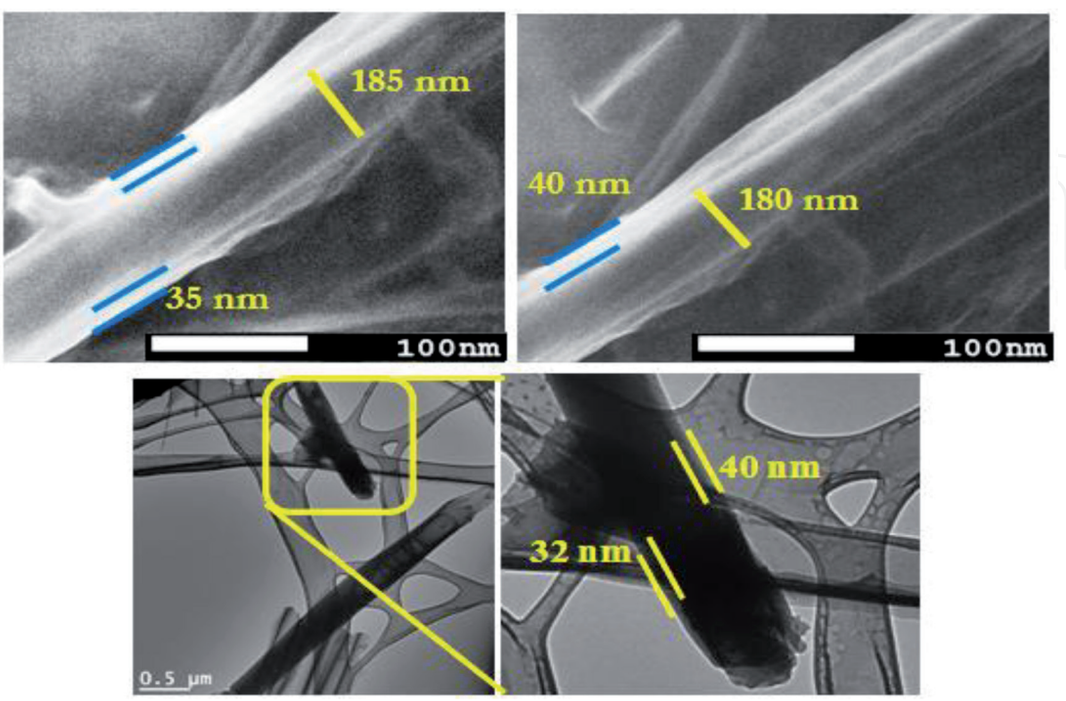

Figure 2.
Selection of SEM and TEM images of coaxial nanowires based on PVK and PPV polymers of an isolated NW which reveals the coaxial geometry.

Generally, this strategy promotes complex phenomena occurring when two (or more) kinds of emitters are into contact, that are Dexter and Förster energy transfers as well as charge transfers. The first mechanism is the energy transfer between PVK and PPV. The emission spectrum of PVK has some overlap with the absorption spectrum of PPV. The spectral overlap is large enough for the efficient energy transfer according to the Forster theory [21]. The energy transfer process from PVK to PPV enhances the PL intensity of PPV.

Here, an energy transfer was accrued between two luminophores because the absorption band of the PPV unit (green dashed-dot line, peak at 420 nm) has a significant overlap with the emission band of the PVK (blue line, peak at 400 nm) as shown on **Figure 3**. Thus, the absorption by the PPV units of the photons emitted by PVK can significantly occur and make evidence of reabsorption phenomenon (energy transfer). This phenomenon was more clearly visible in the PL spectra as shown in **Figure 4**.

The emissive characteristics of the as-prepared NWs have been investigated by PL spectroscopy with a 2 μm diameter microprobe for pumping at 325 nm along the membrane pores, as show in **Figure 4**. The bleu spectrum is composed of the characteristic PVK PL bands located at 389, 418 and 453 nm [20]. However in the case of the green spectra four bands which constitute the spectrum of the PPV are located at 520 nm, 550, 600 and 650 nm [20]. The obtained spectra of the mixture of [PVK@PPV] traced with magenta lines present a linear combination of the PVK and PPV spectra with a strongest contribution of PPV emission. In fact the intensity of PPV luminophores is triple of PVK emission intensity. It is clearly seen that the intensity of PVK is more than PPV emission intensity of about 1.5 before combined together. After mixing the two luminophores [PVK@PPV] the PPV emission intensity become triple of PVK emission intensity. So adding a type of luminophore witch her emission is overlapping with the absorption of the other luminophore resulting increase in emission of this latter.

The sum of two photoluminescence spectra is accompanied by a strong energy transfer as well as evidence of charge transfer. The emission energy of PVK was reabsorbed by PPV units which amplified the PPV emission in the mixture [PVK@PPV]. In addition, as previously reported the PVK emission is overlap of PPV absorption and this is leads to a Forster energy transfer [22–26]. In the same regard, we recall that the quantum yield of PL of PPV is more than of PVK. That means that the PPV polymer has more power to create emissive excitons than in

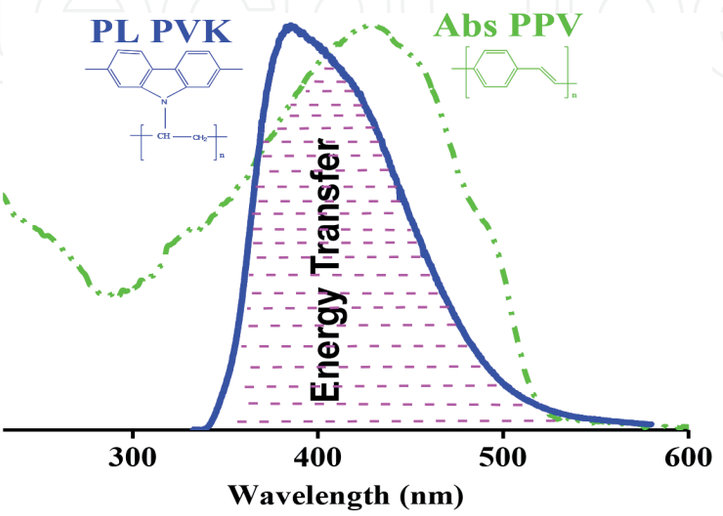

Figure 3.
Normalized absorption (dashed-dot lines), and photoluminescence (solid lines, λexc = 330 nm) spectra of the PVK (blue lines) and of the PPV polymer (green lines).

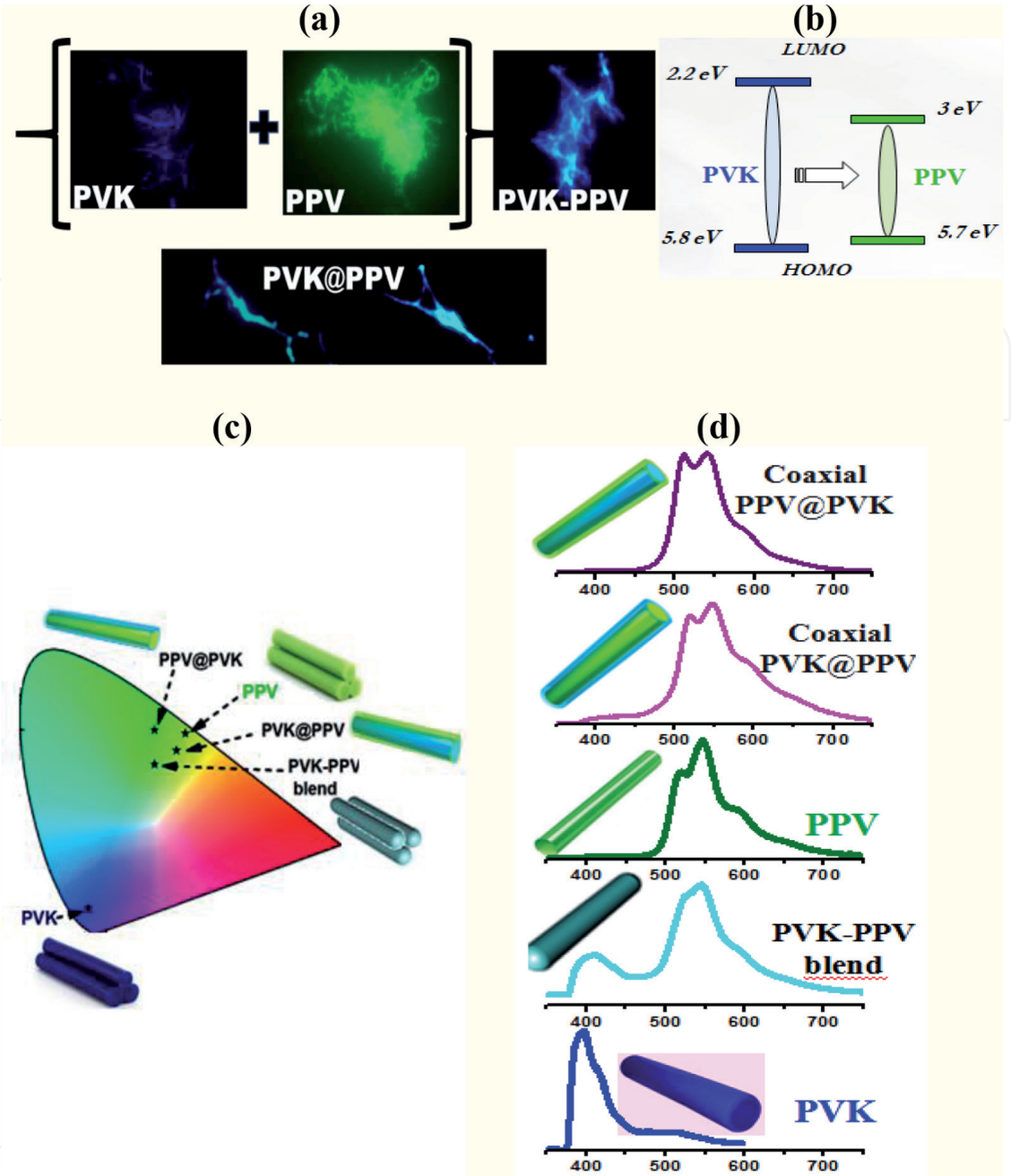

Figure 4.
(a) Fluorescence microscopy images (λexc = 330–380 nm; λem > 420 nm) of dispersed PPV nanowires (green), PVK nanowires (blue) and [PPV@PVK] nanowires (green-bleu) (b) energy transfer phenomena between PVK and PPV (HOMO: Highest occupied molecular orbital, LUMO: Lowest unoccupied molecular orbital); (c) chromaticity diagram (CIE coordinates) for PVK (x = 0.1575; y = 0.0814), PPV (x = 0.3787; y = 0.5919) and [PVK@PPV] (x = 0.3091; y = 0.4968) nanowires LEDs described; (d) photoluminescence (solid lines, laser λexc = 325 nm) spectra of the PVK nanowires (blue lines), PPV nanowires (green lines) and [PPV@PVK] nanowires (magenta lines).

the case of PVK. This is evidence of charge transfer between PPV and PVK units. For charge transfer phenomenon, a similar distance between the donor and the acceptor is needed. Concerning Förster energy transfer, the process is efficient for typical distances 5–10 nm between the donor and the acceptor [26].

Figure 4 shows epi-fluorescence micrographs of random PVK NWs, PPV NWs [PVK@PPV] blend nanowires and coaxial nanowires. A green emission of PPV, blue emission and a bright blue-green characteristic of PPV and PVK emissions are observed in the case of mixture [PVK@PPV]. The color emission corresponding to each PL spectrum has been determined for PVK, PPV and [PVK@PPV] nanowires and reported in a chromaticity diagram. The coordinates of PVK NWs

(x = 0.1575; y = 0.0814), PPV NWs (x = 0.3787; y = 0.5919) and [PVK@PPV] NWs LEDs are displayed in **Figure 4**. It can be noted that the perception of the emission color for the mixture NWs [PVK@PPV] was dominated by the PPV one. Moreover, the contribution of the PPV emission is favored by the higher quantum yield of PPV.

The effect of the coaxial morphology on energy transfer dynamics is now examined. It has been investigated by time-resolved photoluminescence of PVK and PPV thin films, blended and coaxial PVK/PPV nanowires for an excitation at 3.10 eV (400 nm). The nanowires were dispersed on a silica substrate after the total etching of the template. Furthermore, the energy transfer dynamics was investigated by time resolving the PVK, PPV and [PVK@PPV] nanowires optical emission upon excitation at 3.10 eV (400 nm).

Due to the very weak signal measured in the spectral range of PVK emission and of the proximity of the excitation at 400 nm, it was not possible to address the dynamics of the main photoluminescence band. So, we focused on the emission at 535 nm, because it corresponds to the second emission band in the PL tail of PVK, and it is close to the PL maximum of PPV spectrum. Its dynamic behavior is thus expected to take into account the behavior of each polymer and an eventual donor-acceptor mechanism.

Figure 5 depicts the 535 nm PL intensity decays of all the systems investigated in this study. These PL kinetics are simulated with two exponential decays with characteristic time $\tau 1$ and $\tau 2$. In this simple model, the populations of levels 1 and 2 are independent. These populations include photogenerated charges recombining radiatively and non-radiatively. The decaying population is $n = A_1 n_1 + A_2 n_2$, where A1 and A2 are proportional to the PL intensity from levels 1 and 2, respectively [27]. The intensity averaged decay time τ_{mean} has been determined in order to show the average trend of the photogenerated charge migration time. The corresponding decay times and corresponding yields Pi defined as $P_i(\%) = A_i \tau_i / \sum_{i=1}^{2} A_i \tau_i$ are compiled in the **Table 1**.

A first analysis shows that the decays for the blend and the core-shell nanowires are in-between the decay of pure PPV (the faster) and PVK (the slower) decays. The corresponding average decay times are longer (183, 158 and 176 ps) than for

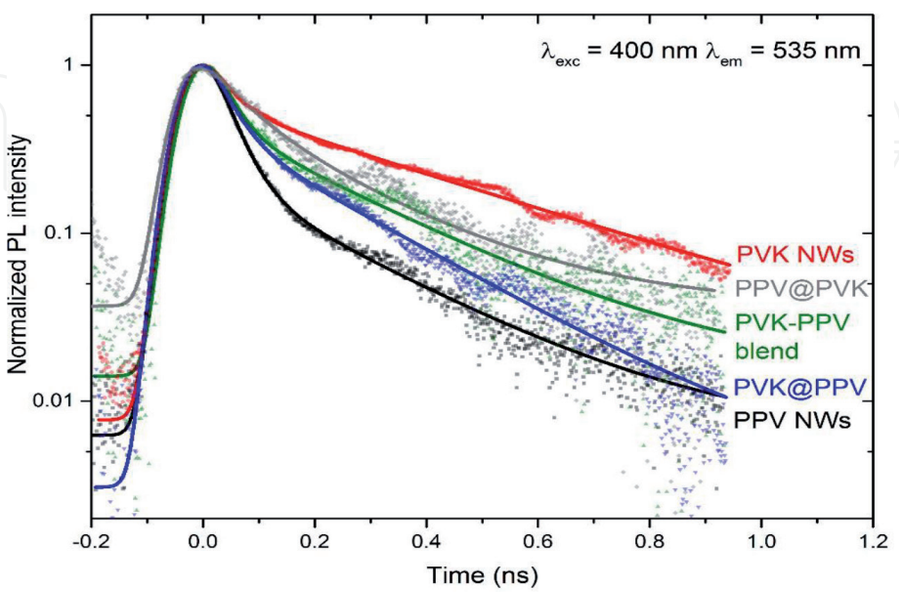

Figure 5.
Normalized photoluminescence decay curves of PVK (red) and PPV (black) nanowires, PVK-PPV blend nanowires (green), and coaxial PPV@PVK (gray) and PVK@PPV (blue) nanowires, extracted for PL emission intensity at 535 nm (excitation wavelength: 400 nm).

Nanowire material	τ_1[a] (ps)	τ_2[b] (ps)	P_1[c] (%)	P_2[d] (%)	τ_{mean}[e] (ps)
PPV	35	238	0.59	0.41	118
PVK	37	405	0.17	0.83	342
PPV-PVK blend	33	254	0.32	0.68	183
PVK@PPV	35	230	0.37	0.63	158
PPV@PVK	67	221	0.29	0.71	176

[a]*Lifetime of the photo-generated charge in the level 1.*
[b]*Lifetime of the photo-generated charge in the level 1.*
[c]*Weight relative of population of photo-generated charges contributing to level 1.*
[d]*Weight relative of population of photo-generated charges contributing to level 1.*
[e]*Average decay time.*

Table 1.
Photoluminescence decays times (in picosecond, with error bars estimated at about 10%) and yields of each component determined from the PL decays shown in ***Figure 5****.*

pristine PPV (τ_{mean} = 118 ps) and shorter than for pristine PVK (τ_{mean} = 342 ps). It can be noted that at an emission wavelength of 535 nm, whatever the kind of nanowires, blend or coaxial, the PL of the PPV component dominates because PPV has the shortest lifetime and a quantum yield slightly larger. In one hand, the system which shows the decay closer to PVK is PPV@PVK. Its longer average lifetime can be attributed to the photogenerated excitons in the PVK when considered as a donor. They have an important probability to diffuse to the acceptor PPV and to transfer their energy before any radiative recombination. In another hand, the system which shows the decay closer to PPV is PVK@PPV. It suggests that the emission by the PPV shell is due to the excitation of PPV excitons partly by the laser probe, and partly by the energy transfer from the photogenerated excitons in the PVK acting as a donor. The case of PVK-PPV blend decay is intermediate between the two coaxial configurations, a bit closer from the PVK@PPV arrangement. It suggests that for this blend, PPV and PVK segments do not deeply affect the exciton dynamics of each other, as expected when chains of both polymers are not entangled, or at least close enough.

These results strongly support the analysis and the conclusion of the steady-state PL study, dominated by morphological issues in relation with the exciton diffusion length of PVK: thin PVK shell for the PPV@PVK nanowires, large PVK diameter for PVK@PPV nanowires, large PVK domains due to a poor intermixing between PPV and PVK obtained during the blending process. This work opens the way to develop alternative solution processing techniques to manage the local organization of donor-acceptor systems at the scale of the exciton diffusion length.

5. Conclusion

In this work, the template method with in-solution processes was exploited to control the respective organization of two polymers at the nanoscale in order to tune the donor-acceptor behavior, and then the photoluminescence properties of such nanowires. Two luminophores, PPV and PVK, were used for the fabrication of coaxial architectures and blend arrangement. The analysis of both steady-state and time-resolved photoluminescence study were analyzed by comparing the exciton diffusion length to the domain size of the nanowire shell,

the nanowire core, or the segregated domains in the blend case. Charge and energy transfer process occurred in these coaxial NWs are more described using stationary and time resolving photoluminescence. These coaxial morphology based to PVK and PPV polymers showed an amplified of emission PPV intensity by adding PVK.

Acknowledgements

The authors would like to thank these colleagues at the Institute of Materials Jean Rouxel in Nantes: Jean-Luc duvail, Florian Massuyeau and Eric Faulques for help in optical study.

Author details

Mohamed Mbarek* and Kamel Alimi
Laboratory Research: Assymetric Synthesis and Molecular Engineering of New Materials for Organic Electronic (LR18ES19), Faculty of Sciences Monastir, Tunisia

*Address all correspondence to: mohamedmbarek99@yahoo.fr

References

[1] Choi M, Kim Y, Ha C. Polymers for flexible displays: From material selection to device applications. Prog. Polym. Sci. 2008;33:581-630 . https://doi.org/10.1016/j.progpolymsci.2007.11.004

[2] Chen S, Li Y, Li Y,Architecture of low dimensional nanostructures based on conjugated polymers. Polym Chem. 2013 ;4 :5162-5180 https://doi.org/10.1039/C3PY00098B

[3] Shane M, Pierre L, Deirdre O'C, Daniela I, Gareth R. Alignment and Dynamic Manipulation of Conjugated Polymer Nanowires in Nematic Liquid Crystal Hosts. Advanced Materials 2008;20:2497-2502. https://doi.org/10.1002/adma.200701986

[4] Lang J, Huanli D, Wenping H. Controlled growth and assembly of one-dimensional ordered nanostructures of organic functional materials Soft Matter, 2011;7:1615-1630

[5] Li X, Wang T, Zhang J, Zhu D, Zhang X, Ning Y, Zhang H, Yang B. Controlled Fabrication of Fluorescent Barcode Nanorods. ACS Nano 2010;4:4350-4360. https://doi.org/10.1039/C0SM00762E

[6] Park D.H, Hong Y.K, Cho E.H, Kim M.S, Kim D.C, Bang J, Kim J, Joo J, Light-Emitting Color Barcode Nanowires Using Polymers: Nanoscale Optical Characteristics. ACS Nano 2010;4:5155-5162. https://doi.org/10.1021/nn101096m

[7] Gu F, Zhang L, Yin X, Tong L. Polymer Single-Nanowire Optical Sensors. Nano Lett. 2008;8:2757-2761. https://doi.org/10.1021/nl8012314

[8] Zhao Y.S, Wu J, Huang J. Vertical Organic Nanowire Arrays: Controlled Synthesis and Chemical Sensors. J. Am. Chem. Soc. 2009;131:3158-3159. https://doi.org/10.1021/ja809360v

[9] Zang L, Che Y, Moore J.S. One-Dimensional Self- Assembly of Planar pi-Conjugated Molecules: Adaptable Building Blocks for Organic Nanodevices. Acc. Chem. Res. 2008;41:1596-1608. https://doi.org/10.1021/ar800030w

[10] Mbarek M, Garreau A, Massuyeau F, Alimi K, Wéry J, Faulques E, Duvail. J.L. Template process for engineering the photoluminescence of PVK and PPV-based nanowires". Journal of Apllied Polymer Sciences 2019;136:48201. https://doi.org/10.1002/app.48201

[11] Garreau A, Massuyeau F, Cordier S, Molard Y, Gautron E, Bertoncini P, Faulques E, Wery J, Humbert B, Bulou A, Duvail J-L. Color Control in Coaxial Two-Luminophore Nanowires ACS Nano 2013 ;7:2977-2987. https://doi.org/10.1021/nn400763r

[12] Che Y, Yang X, Loser S, Zang L. Expedient Vapor Probing of Organic Amines Using Fluorescent Nanofibers Fabricated from an n-Type Organic Semiconductor. Nano Lett. 2008;8:2219-2223. https://doi.org/10.1021/nl080761g

[13] O'Carroll D, Lieberwirth I, Redmond,G. Microcavity Effects and Optically Pumped Lasing in Single Conjugated Polymer Nanowires. Nat. Nanotechnol. 2007;2:180-184. https://doi.org/10.1038/nnano.2007.35

[14] Zhao Y.S, Peng A, Fu H, Ma Y, Yao J. Nanowire Waveguides and Ultraviolet Lasers Based on Small Organic Molecules. Adv. Mater. 2008;20:1661-1665. https://doi.org/10.1002/adma.200800123

[15] Kuo C.C, Lin C.H, Chen W.C. Morphology and Photophysical Properties of Light-Emitting Electrospun Nanofibers Prepared from Poly(fluorene) Derivative/PMMA Blends. Macromolecules

2007;40:6959-6966. https://doi.org/10.1021/ma071182l

[16] Yang H, Lightner C.R, Dong L. Light-Emitting Coaxial Nanofibers. ACS Nano 2012;6:622-628. https://doi.org/10.1021/nn204055t

[17] Zhao Y.S, Fu H.B, Hu F.Q, Peng A.D, Yang W.S, Yao J.N. Tunable Emission from Binary Organic One-Dimensional Nanomaterials: An Alternative Approach to White-Light Emission. Adv. Mater. 2008;20:79-83. https://doi.org/10.1002/adma.200890030

[18] Simbrunner C, Hernandez-Sosa G, Quochi F, Schwabegger G.N, Botta C, Oehzelt M, Salzmann I, Djuric T, Neuhold A, Resel R, Color Tuning of Nanofibers by Periodic Organic-Organic Hetero-Epitaxy. ACS Nano 2012;6:4629-4638. https://doi.org/10.1021/nn2047235

[19] Lakowicz J.R, Principles of Fluorescence Spectroscopy, 3rd ed.; Springer: New York, 2006. https://www.springer.com/gp/book/9780387312781

[20] Mbarek M, Massuyeau F, Duvail J.L, Wéry J, Faulques E, Alimi K. New copolymer of poly (N-vinylcarbazole) and poly (p-phenylenevinylene) for optoelectronic devices. Journal of Apllied Polymer Sciences 2013;130:2839-2847), DOI: 10.1002/app.39496.

[21] Chi-Jung C, Yao-Yi C, Min Huei W, Chi Shen T. Miscibility effect on the energy transfer induced luminescence enhancement of polyimide/PVK blends Thin Solid Films 2005;477:14-18. https://doi.org/10.1016/j.tsf.2004.08.104

[22] Dennis A.M, Bao G. Quantum Dot-Fluorescent Protein Pairs as Novel Fluorescence Resonance Energy TransferProbes. Nano Lett. 2008;8:1439-1445. https://doi.org/10.1021/nl080358+

[23] Stoferle T, Scherf U, Mahrt R.F. Energy Transfer in Hybrid Organic/Inorganic Nanocomposites. Nano Lett. 2009;9:453-456. https://doi.org/10.1021/nl8034465

[24] Bredas J.L, Beljonne D, Coropceanu V, Cornil J. Charge- Transfer and Energy-Transfer Processes in pi-Conjugated Oligomers and Polymers: A Molecular Picture. Chem. Rev. 2004;104:4971-5003. https://doi.org/10.1021/cr040084k

[25] Forster, T. Transfer Mechanisms of Electronic Excitation. Discuss. Faraday Soc. 1959;27:7-17. https://doi.org/10.1039/DF9592700007

[26] Halivni S, Sitt A, Hadar I, Banin U, Effect of Nanoparticle Dimensionality on Fluorescence Resonance Energy Transfer in Nanoparticle-Dye Conjugated Systems. ACS Nano 2012;6:2758-2765. https://doi.org/10.1021/nn300216v

[27] Mohamed M, Lamia S, Kamel A, New copolymer involving PVK and F8BT for organic solar cells applications: Design, synthesis, characterization and theoretical studies". Optical Materials 2019;91:447-454. https://doi.org/10.1016/j.optmat.2019.03.053